

PAPER

## Quantitative analysis of recombinant glucocerebrosidase brain delivery via lipid nanoparticles

To cite this article: Meir Goldsmith *et al* 2018 *Nano Futures* **2** 045003

View the [article online](#) for updates and enhancements.



**IOP | ebooks™**

Bringing you innovative digital publishing with leading voices to create your essential collection of books in STEM research.

Start exploring the collection - download the first chapter of every title for free.



## PAPER

## Quantitative analysis of recombinant glucocerebrosidase brain delivery via lipid nanoparticles

RECEIVED  
30 June 2018ACCEPTED FOR PUBLICATION  
28 August 2018PUBLISHED  
10 September 2018Meir Goldsmith<sup>1,2,3,4,5</sup>, Lilach Abramovitz<sup>1,2,3,4,5</sup>, Hila Braunstein<sup>2</sup>, Mia Horowitz<sup>2,6</sup> and Dan Peer<sup>1,2,3,4,5,6</sup> <sup>1</sup> Laboratory of Precision NanoMedicine, Tel Aviv University, Tel Aviv 69978, Israel<sup>2</sup> Department of Cell Research & Immunology, George S Wise Faculty of Life Sciences, Tel Aviv University, Tel Aviv 69978, Israel<sup>3</sup> Department of Materials Sciences and Engineering, Iby and Aladar Fleischman Faculty of Engineering, Tel Aviv University, Tel Aviv 69978, Israel<sup>4</sup> Center for Nanoscience and Nanotechnology, and Tel Aviv University, Tel Aviv 69978, Israel<sup>5</sup> Cancer Biology Research Center, Tel Aviv University, Tel Aviv 69978, Israel<sup>6</sup> Authors to whom any correspondence should be addressed.E-mail: [horowitzm@post.tau.ac.il](mailto:horowitzm@post.tau.ac.il) and [Peer@tauex.tau.ac.il](mailto:Peer@tauex.tau.ac.il)

Keywords: lipid nanoparticles, case, brain delivery

**Abstract**

Gaucher disease (GD), the most prevalent genetic lysosomal storage disease, is characterized by the accumulation of glucosylceramide, mainly in monocyte-derived cells, due to deficient activity of lysosomal acid- $\beta$ -glucocerebrosidase (GCase). The disease is heterogeneous and may vary from a very mild visceral disease to a severe neuronopathic disease, with very early death during the first years of life. Two therapeutic modalities are in use today; enzyme replacement therapy (ERT) and substrate reduction therapy (SRT). Neither of the two modalities are applicable for patients with the neuronopathic forms of GD. While the infused enzyme in ERT cannot cross the blood–brain-barrier, SRT is not suitable for young patients. Herein, we investigated novel approaches to deliver recombinant GCase (rGCase) into the brain using lipid nanoparticles (LNPs). These LNPs were composed of a mixture of negative, positive and zwitterion phospholipids and were delivered intranasally into the brains of mice. A quantitative analysis performed intranasally in mice revealed a dramatic accumulation of the enzyme that was formulated into the LNPs in the brains of the mice ( $3.91\% \pm 0.3\%$  injected dose (ID)/mg tissue) versus the free enzyme ( $0.29\% \pm 0.07\%$  ID/mg tissue). The administrated particle-delivered enzymes were able to enter the brain parenchyma and accumulate in the CD11b<sup>+</sup> cells, which are the target cells in GD. When supplied to GD-derived skin fibroblasts, a  $35\% \pm 1.2$  increase in intracellular GCase activity was measured only with the LNP-encapsulated enzyme. This strategy may pave the way for novel therapeutic modalities to treat GD and other diseases such as Alzheimer's and Parkinson's.

**1. Introduction**

Gaucher disease (GD) is an autosomal recessive lysosomal storage disorder caused by defects in the *GBA1* gene, encoding acid  $\beta$ -glucocerebrosidase (GCase) [1, 2]. Decreased GCase activity leads to the accumulation of glucosylceramides, mainly in monocyte-derived lineages [3]. GCase accumulation can manifest in a variety of phenotypes ranging from a perinatal lethal form to an asymptomatic form [4, 5]. Due to its heterogeneity, GD has been divided into three clinical types based on disease phenotype, progression and the presence or absence of neurological involvement. The most prevalent type, 1 GD, is essential non-neuropathic since it lacks primary central nervous system (CNS) involvement. Patients with this type of disease may develop anemia, thrombocytopenia, hepatosplenomegaly, skeletal abnormalities, interstitial lung disease and pulmonary hypertension [6]. Type 2 GD is an acute neuropathic form with severe neurological manifestations and survival is limited to the first years of life. Type 3 GD is also characterized by neurological involvement but neurological

symptoms generally appear later in life in comparison to type 2, and include abnormal eye movements, ataxia, seizures, and dementia, with patients surviving until their 30s or 40s [7].

To date there are two therapeutic modalities for GD, enzyme replacement therapy (ERT) and substrate reduction therapy (SRT). ERT has emerged as the standard of care for type I GD [8, 9]. Over two decades since the introduction of this therapy [10], it has become clear that many of the symptoms and signs of visceral GD respond adequately to ERT [11]. Despite its great success, ERT also has disadvantages, including costly manufacture, inconvenience of the intravenous infusions and the inability of the intravenously administered enzyme to cross the blood–brain barrier (BBB).

In the present study, we aimed to develop an approach, which will facilitate the administration of recombinant GCase (rGCase) into the CNS while bypassing the BBB. In order to achieve this, we devised a carrier that encapsulated the rGCase and utilized an alternative delivery method into the brain. We focused on lipid nanoparticles (LNPs) as the vehicles for protein delivery since LNPs have been shown to successfully encapsulate a wide variety of proteins including superoxide dismutase [12], acetylcholinesterase [13] and myoglobin [14] and were successful in protecting protein cargo from environmental factors and degradation [15–18]. LNPs also facilitate tissue and cellular penetration primarily by the endocytic pathway, due to the lipophilic nature of LNPs [19]. Furthermore, LNPs have been used for the transport of anticancer and anti-inflammatory drugs into the brain by intravenous [20] or intracerebral delivery [21]. LNPs are easily modified by changing the composition of the phospholipids. Such modifications enable a wide range of possibilities to suit encapsulation of different proteins and facilitate cellular penetration [22].

Crossing the BBB and reaching the desired destination in the brain depends not only on the composition of the carriers but also on the routes of administration. Herein we focused on the intranasal (IN) delivery route. IN mediated delivery of proteins has emerged as a non-invasive, safe and effective method to target peptides and proteins to the CNS, bypassing the BBB, minimizing systemic exposure and limiting peripheral adverse effects [23].

## 2. Materials and methods

### 2.1. LNP preparation

1,2-Dilauroyl-sn-glycero-3-phosphorylethanolamine (DLPE), 1,2-Dilauroyl-sn-glycero-3-phosphorylglycerol (DLPG) and 1,2-di-O-octadecenyl-3-trimethylammonium propane (DOTMA) were purchased from Avanti Polar Lipids Inc. (AL USA). The lipids were dissolved in ethanol and mixed together at three different molar ratios, either 60:40 (DLPE/DLPG), 57.5:37.5:5 (DLPE/DLPG/DOTMA) or 52.5:32.5:15 (DLPE/DLPG/DOTMA). The solution was evaporated until dry under a reduced pressure in a Buchi Rotary Evaporator Vacuum System (Flawil, Switzerland) and hydrated with either 50 mM citrate buffer (pH 6) or 50 mM citrate buffer (pH 6) with rGCase ( $1 \text{ mg ml}^{-1}$  rGCase) to a final concentration of  $5 \text{ mg ml}^{-1}$  lipids and shaken for 2 h at room temperature. After being kept overnight at  $4^\circ\text{C}$  the LNPs were extruded through a Lipex Extrusion Device (Northern lipids, Vancouver, Canada), operated under nitrogen pressures of 200–500 psi with a filter pore size of 400 nm (Whatman Inc., UK). The LNPs were dialyzed three times in acetate buffer (pH = 6, 50 mM) using the Float-A-Lyzer 1000 kD dialysis system (Spectrum Labs, CA, USA) to remove unencapsulated rGCase. For fluorescent labeling of the rGCase we used the Alexa-647 labeling kit #120173 from molecular probes (molecular probes, Thermo Fisher Scientific, MA, USA) in accordance with the manufacturer's protocol. The final protein to fluorophore ratio was 1:3.6 as determined by the nanodrop ND-2000 UV–vis spectrophotometer assessment (Thermo Fisher Scientific, MA, USA).

### 2.2. rGCase radiolabeling

Recombinant glucocerebrosidase was tritiated in the presence of a palladium-charcoal catalyst as previously shown [24] glucocerebrosidase activity was found to be  $4.3 \times 10^6$  dpm/nmol by thin-layer chromatography. [ $^3\text{H}$ ] Glucocerebrosidase ( $0.2 \times 10^6$ – $4 \times 10^6$  dpm, 0.047–0.093 nmol), 25  $\mu\text{g}$  Triton X-100, 93 nmol sodium taurocholate, and 28 nmol palmitoylglucocerebrosidase were solubilized as described above, in 50–1.0  $\text{mol l}^{-1}$  sodium citrate buffer (pH 5.6).

### 2.3. Protein encapsulation efficiency

LNPs with or without rGCase were incubated in PBS containing 1% sodium deoxycholate. After 30 min of agitation the LNPs were centrifuged three times in a 10 k centricon (Millipore Ireland BV). The discarded liquid was replaced with PBS 1% sodium deoxycholate. The samples were incubated for 10 min between each centrifugation. The LNP remanences were dialyzed three times in 12 kD dialysis tubes (GEBA, Israel) in PBS to remove the sodium deoxycholate.

Protein levels were evaluated with the BCA protocol (Pierce, Thermo Fisher Scientific) in accordance with manufacturer's instructions. Free GCCase was used to create the standard curve.

#### 2.4. LNP size distribution and zeta potential measurements

LNP size distribution and zeta potential were measured on a Malvern Zetasizer Nano ZS Zeta Potential and DLS instrument (Malvern Instruments, Southborough, MA, USA) using the automatic algorithm mode and analyzed with the PCS 1.32a. All size measurements were done in 50 mM, pH 6 acetate buffer, at room temperature.

#### 2.5. Electron microscopy

The structure of the LNPs with or without rGCCase was investigated using TEM. Samples were adsorbed on Formvar/carbon-coated grids and negatively stained with 2% aqueous uranyl acetate. Samples were examined using a Jeol 1200EX TEM (Jeol, Japan).

#### 2.6. Internalization assays

All single cell suspensions were obtained with the MACS Dissociator (Miltenyl Biotec) using the Neural Tissue Dissociation Kit (Miltenyl Biotec) according to manufacturer's instructions. Myelin removal was performed by centrifugation in a percoll gradient (Sigma, Israel).

For *ex vivo* LNP administration: single cell suspensions from mouse brains were seeded on 35 mm plates (IBIDI GmbH, Germany) and grown in RPMI medium supplemented with antibiotics, L-Glutamine and 10% fetal calf serum (Biological industries, Beit Haemek, Israel). After 24 h the cells were exposed to LNPs in serum-free medium for 2 h at 37 °C in a humidified atmosphere with 5% CO<sub>2</sub>, and subsequently the cells were washed twice with PBS.

For IN administration of the LNPs: single cell suspensions from treated and untreated mice were seeded on 35 mm plates (IBIDI GmbH, Germany) in PBS and were kept at 4 °C.

Prior to confocal microscopy, the cells were incubated with 488-Alexa conjugated anti-CD11b antibodies (BioLegend), with LysoTracker<sup>®</sup> Red DND-99 (Thermo Fisher Scientific) as a lysosome marker and with Hoechst (SIGMA, Israel) for nuclear staining. Confocal microscope images were obtained on live cells using the Nikon Eclipse C2 configured with a NI-E microscope and processed with NIS-elements software using X60 objective magnification (Nikon).

#### 2.7. Mice

The mice were housed and maintained in laminar flow cabinets under specific pathogen-free conditions in the animal quarters of Tel Aviv University and in accordance with current regulations and standards of the Israel Ministry of Health. All animal protocols were approved by Tel Aviv University Institutional Animal Care and Use Committee.

#### 2.8. IN administration, radioactivity analysis and IVIS imaging

Eight week old BALB/C female mice (Envigo Laboratories) were anesthetized with a subcutaneous injection of Ketamine/Xylazine solution (100 mg kg<sup>-1</sup> Ketamine, 10 mg kg<sup>-1</sup> Xylazine). Free rGCCase, enzyme-free LNPs or encapsulated rGCCase (1 mg ml<sup>-1</sup>) were administered intranasally at a volume of 25 µl/animal, alternating between the nostrils. After administration the mice were left to recuperate before being returned to their cage. *In vivo* imaging was performed using the IVIS 2000 *in vivo* imaging system (Caliper Life Sciences, Hopkinton, MA, USA). For radioactivity analysis, free <sup>3</sup>H-rGCCase was assayed using an EnVision Multimode Plate Reader (PerkinAlmer).

#### 2.9. Cell model for GD

Human primary skin fibroblasts (cultured fibroblasts) were from NIGMS Human Genetic Cell Repository (cell lines: GM8760, L444P/L444P and GM877, L444P/RecNciI). The cells were grown in DMEM supplemented with 20% FBS (Biological Industries, Beit Haemek, Israel), at 37 °C in the presence of 5% CO<sub>2</sub>.

#### 2.10. Enzymatic activity

Confluent primary skin fibroblasts incubated for 4 h with 100 µg of different formulations of rGCCase were washed twice with ice-cold PBS and collected in 150 µl sterile water. Cell lysates, containing 40 µg of protein, were assayed for GCCase activity in 0.2 ml of 100 mM potassium phosphate buffer, pH 4.5, containing 0.15% Triton X-100 (Sigma, Israel) and 0.125% taurocholate (Calbiochem, La Jolla, CA, USA) in the presence of 1.5 mM 4-MUG (Genzyme Corp. Boston, MA, USA) for 1 h at 37 °C. The reaction was stopped by the addition of 0.5 ml of stop solution (0.1M glycine, 0.1M NaOH, pH10) and the amount of 4-methyl-umbeliferone (4-MU)

**Table 1.** Physicochemical and structural analysis of lipid nanoparticles (LNPs). (A) Hydrodynamic diameters and zeta potential measurements of the different LNPs. (B) Enzyme encapsulation within LNPs and enzymatic activity relative to free enzyme.

(A)		
LNPs—lipid content	Size (nm)	Zeta (mv)
DLPE-DLPG	209.8 ± 2.15	−117.3
DLPE-DLPG 5% DOTMA	219.1 ± 4.81	−93.3
DLPE-DLPG 15% DOTMA	225.9 ± 3.27	−84.2
DLPE-DLPG 647-Gcase	193.2 ± 4.89	−74.1
DLPE-DLPG 5% DOTMA 647-Gcase	148.6 ± 4.85	−71.8
DLPE-DLPG 15% DOTMA 647-Gcase	220.1 ± 5.13	−79.7
(B)		
LNPs content	Encapsulation (%)	Enzyme activity (%)
DLPE-DLPG + rGCCase	9.98 ± 0.39	94 ± 1.7
DLPE-DLPG + 15% DOTMA + rGCCase	8.7 ± 0.35	99 ± 0.2

was quantified using a Perkin Elmer Luminescence Spectrometer LS 50 (excitation length: 340 nm; emission: 448 nm).

### 2.11. Statistical analysis

All data are expressed as a mean with SEM in animals and with SD for *in vitro* and physicochemical characterization of the delivery system. The comparison of the two experimental groups was performed using two-sided Student t-test. Analyses were performed with Prism 7 (Graphpad Software). Differences are labeled n. s. for not significant, \* for  $p \leq 0.05$ , \*\* for  $p \leq 0.01$ , and \*\*\* for  $p \leq 0.001$ . The sample size of each experiment was determined to be the minimum necessary for statistical significance by the common practice in the field. No animals were excluded from the experiments.

## 3. Results

### 3.1. Preparation and characterization of lipid NPs containing rGCCase

Since the accumulation of glucosylceramides characterizes macrophage derived cells, it is obvious that microglia cells are the target for ERT in neuronopathic GD [25, 26]. Although microglia and other macrophage cells readily phagocytose LNPs [27], we wanted to augment this processes in order to improve protein delivery. Previous reports have demonstrated that phagocytosis can be amplified by altering the size and charge of the particle. For example, by increasing the negative charge of the LNPs, superior phagocytosis was observed [27, 28]. Based on this finding we designed our nanocarriers to include the phospholipid DLPG, which is negatively charged and is known to facilitate macrophage phagocytosis [27]. We also used the lipid DLPE, which is known to destabilize the particles and enhance penetration into cells [29, 30]. Additional formulations that were examined incorporated the cationic lipid DOTMA. We chose to use DOTMA as the permanent charged cationic lipid, as it has been shown to enable cellular penetration and enhance drug delivery [31]. Intracellular targeting is not a concern for ERT in GD as phagocytosed particles are quickly shuttled to the lysosome [32], which is the intracellular site of action of GCCase in normal cells.

rGCCase was entrapped within LNPs constructed of the lipids DLPE and DLPG, at a mole ratio of 3:2, with or without the cationic lipid DOTMA (5% and 15%), as detailed in the Materials and Methods section (section 2). The particles were analyzed for size distribution using dynamic light scattering (DLS) and zeta potential using a zeta sizer (table 1).

GCCase encapsulation in all particle formulations showed significant increase in the zeta potential to a zeta of  $\sim -75$  mv. This increase in zeta potential coupled with the low encapsulation efficiency (of about 10%) could indicate that some of the GCCase was not entrapped within the lipid bilayer but was attached to the surface of the particle as a protein corona; a similar phenomenon of zeta change due to protein corona formation has been documented with other proteins [33, 34]. In addition, such a high zeta potential indicates that the particle will not aggregate. To further elucidate the ultrastructure of the particles, we used transmission electron microscopy (TEM) analysis. The captured images revealed that the particles were of circular shape as expected, with high homogeneity. The size measurement of the particles was in good agreement with the DLS analysis (figure 1). The LNPs without the rGCCase had globular shapes and round surfaces whereas the LNPs containing the rGCCase exhibited flower-like particles.

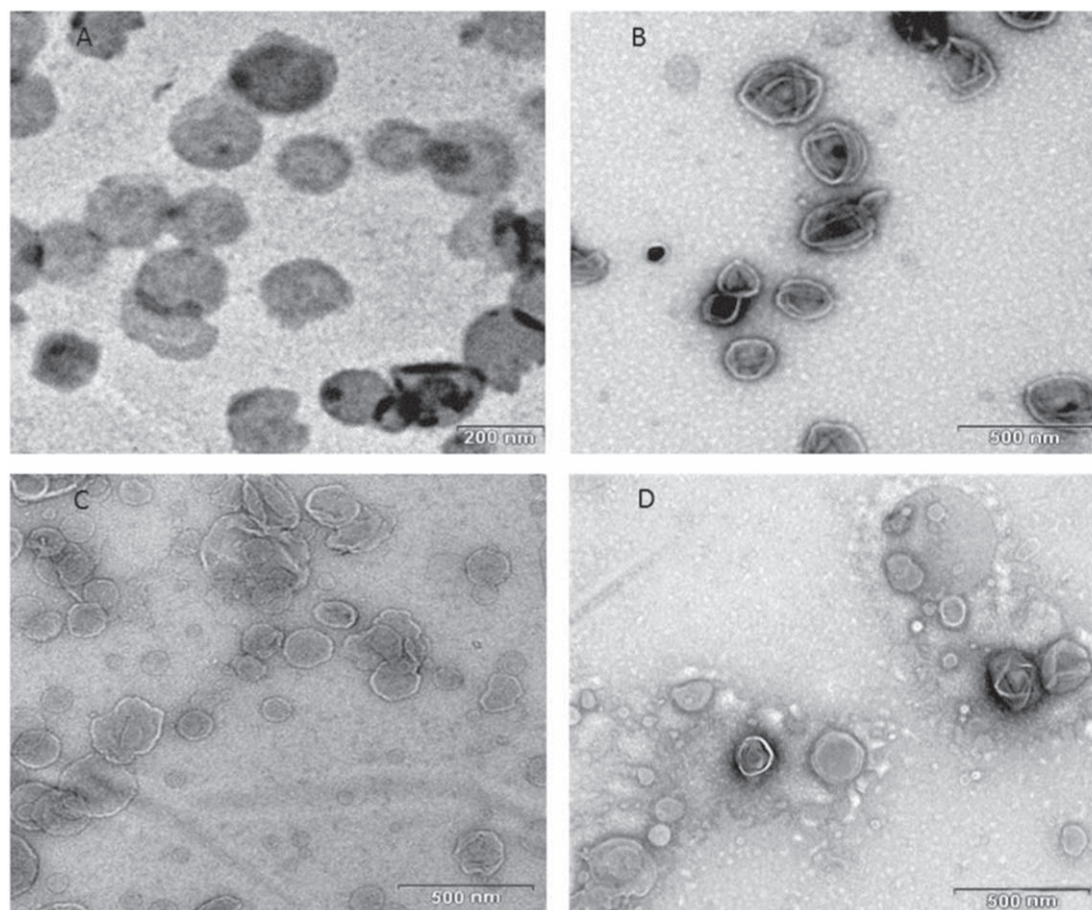


**Figure 1.** Transmission electron microscopy (TEM) analysis of LNPs. Representative images of: (A) DLPE/DLPG only, (B) DLPE/DLPG LNPs with rGCCase (C) DLPE/DLPG which include 5% DOTMA and rGCCase (D) DLPE/DLPG which include 15% DOTMA and rGCCase.

In order to further characterize the LNPs, we analyzed the amount of encapsulated GCCase as described in the Materials and Methods section. The encapsulation efficiency was 8.7% for the DOTMA-containing LNPs and 10% for the DOTMA-free LNPs (table 1). We also determined encapsulation efficiency using the fluorescent emission of an Alexa-647 labeled rGCCase (647-GCCase) with similar results (data not shown). These low encapsulation levels are typical levels for protein entrapment in LNPs however we wanted to determine if these low levels are enough to retain biological activity. To determine if the encapsulated rGCCase retained its enzyme activity, we measured enzymatic activity of free rGCCase and of the encapsulated enzyme using the 4-MUG as a substrate, as described in the Materials and Methods section. Our results demonstrated that the encapsulated enzyme retains its activity during the encapsulation process (table 1). Taken together these results demonstrate that we have constructed stable LNPs that successfully entrapped rGCCase. Moreover, we have demonstrated that the encapsulation procedure did not impair the enzymatic activity of rGCCase.

### 3.2. Internalization of rGCCase containing LNPs into their target cells in the brain

As monocyte-derived cells play a pivotal role in GD and are considered as the target cells for ERT [3], we turned our attention to the resident macrophages of the brain, the microglia cells. To examine the ability of microglia cells to internalize rGCCase, single cell suspension, extracted from the brains of BALB/c mice were treated for 2 h with rGCCase, labeled with the 647-Alexa dye, either as free rGCCase or rGCCase entrapped in LNPs of different formulations. 488-Alexa labeled anti-CD11b antibody was used for microglia staining. Our results (figure 2) revealed that only microglia cells (CD11b<sup>+</sup> cells) were able to internalize both the free and the entrapped rGCCase. The fact that free rGCCase could enter microglia was expected, since the recombinant enzyme is highly mannosylated, and these mannose residues recognize mannose receptor on the cells, through which it is endocytosed [35].

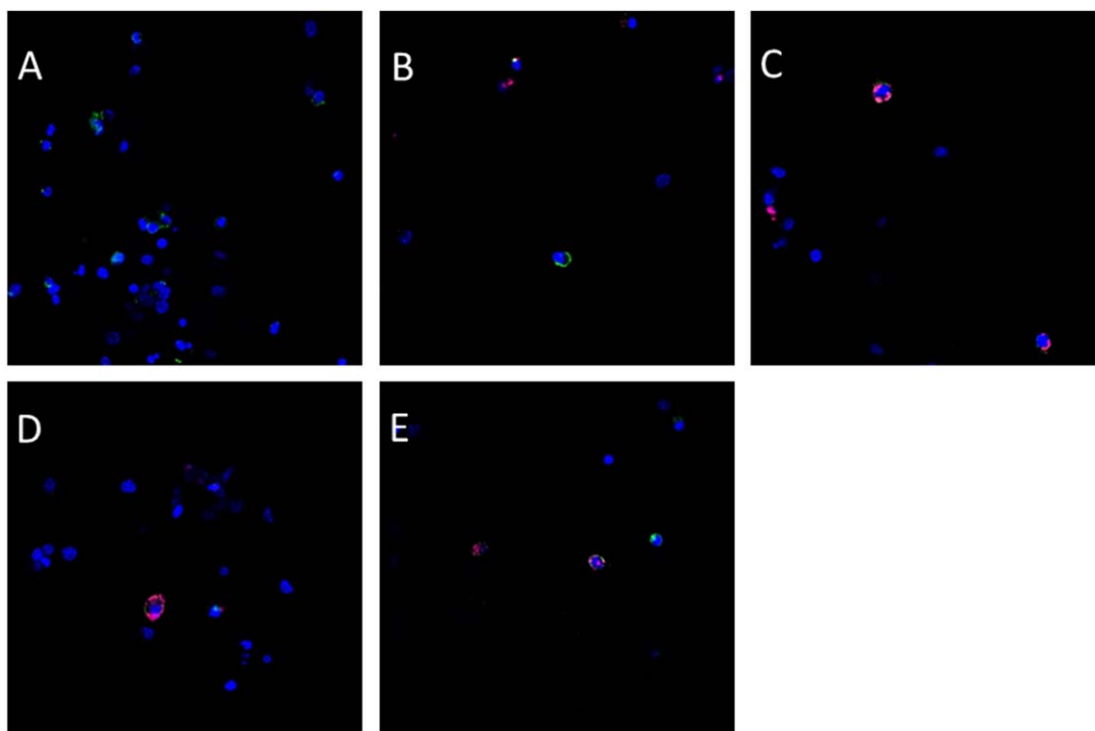


**Figure 2.** Analysis of rGCCase endocytosis. Single cell suspensions were prepared from total brains. The cells were: (A) untreated (B) incubated with Free 647-Alexa-rGCCase (C) incubated with DOTMA-free particles containing 647-Alexa-rGCCase (D) incubated with 5% DOTMA-particles containing 647-Alexa-rGCCase; (E) incubated with 15% DOTMA-particles containing 647-Alexa-rGCCase. Incubation was for 2 h at 37°. Following washes with PBS, the cells were stained with anti-CD11b antibodies (green) and Hoechst for nuclear marker (Blue). 647-Alexa-rGCCase is shown in magenta. The cells were visualized using confocal microscopy.

### 3.3. LNPs entrapping rGCCase delivered the enzyme into the brain via an IN administration route

Treatment of neurodegenerative diseases requires drug delivery to the brain, either by crossing an intact BBB or by bypassing it. *In vivo* experiments in mice were conducted to evaluate the ability of the LNPs to deliver rGCCase to the brain, bypassing the BBB via IN administration. rGCCase (1 mg ml<sup>-1</sup> of 647-Alexa-labeled enzyme) was introduced into eight week old, BALB/c female mice. The experiment was performed with 12 animals, divided into four groups. Each group consisted of three mice receiving a specific treatment: free 647-Alexa-rGCCase, free LNPs, 5% DOTMA-containing LNPs with 647-Alexa-rGCCase and 15% DOTMA-containing LNPs entrapping 647-Alexa-rGCCase. The mice received three daily consecutive treatments via IN administration and 24 h after the final treatment distribution of rGCCase in the brain was determined using the IVIS imaging system. The results (figure 3) showed that both forms (free rGCCase and rGCCase entrapped in the LNPs) entered the brain via the olfactory bulb, with a distinct advantage for the encapsulated rGCCase over the free enzyme. Other groups have shown [36–43] that proteins can be delivered intranasally into the brain, however the same groups reported that some proteins were degraded or incised by nucleases present in the mucosa [44].

We next asked how much enzyme was delivered into the brain in a quantitative manner. We used a labeled <sup>3</sup>H-rGCCase to study the quantitative delivery of the free enzyme versus the entrapped enzyme. We isolated the brain after single administration (corresponding to 0.25 mg ml<sup>-1</sup> of free enzyme or enzyme entrapped in LNPs). We found that the amount reaching the brain with the free enzyme corresponded to 0.29% ± 0.07, % ID/mg tissue whereas the amount of the entrapped enzyme corresponded to a 3.91% ± 0.3% injected dose (ID)/mg tissue. This represents a dramatic delivery of the entrapped enzyme over the free enzyme by more than 10-fold. We next asked what were the target cells that took up the enzyme in the brain.

### 3.4. rGCCase entrapped within LNPs is delivered into microglia lysosomes

BALB/c mice were administered intranasally either with free 647-Alexa-rGCCase or with 647-Alexa-rGCCase, entrapped in one of the LNPs formulations, as described. Twenty-four hours after the third administration, the mice were anesthetized and following perfusion, the brains were homogenized to produce single cell suspension. Cells were stained with 488-Alexa-labeled anti-CD11b antibodies and Red DND-99 LysoTracker® to visualize lysosomes. The results (figure 4) revealed that GCCase was detected only in CD11b positive cells (microglia), which are the target cells of the enzyme. Within the microglia, the rGCCase was located predominately in the lysosomes. In this experiment, contrary to the *ex vivo* results (figure 3), there was a significant difference between

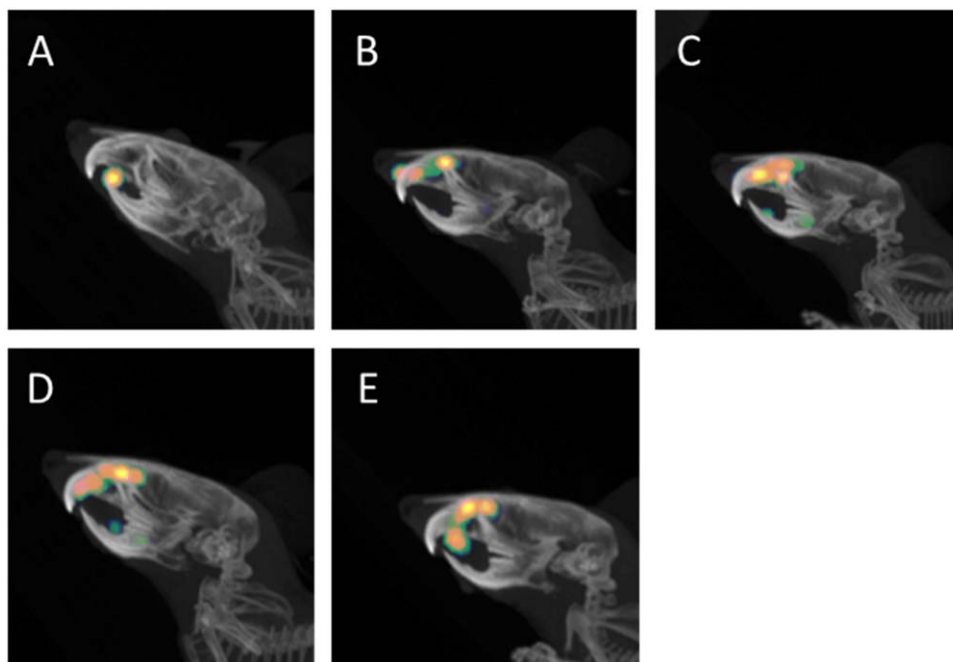


**Figure 3.** Administration of rGCCase into the brain. BALB/c mice were administered an IN dose of 25  $\mu$ g rGCCase in one of the following treatments: (A) mock (no rGCCase) (B) free 647-Alexa labeled rGCCase (C) LNPs with 647-Alexa labeled-rGCCase (D) 5% DOTMA-containing LNPs with 647-Alexa labeled-rGCCase, (E) 15% DOTMA-containing LNPs with 647-Alexa labeled-rGCCase. 24 h after administration, the mice were imaged using the IVIS fluorescent imager.

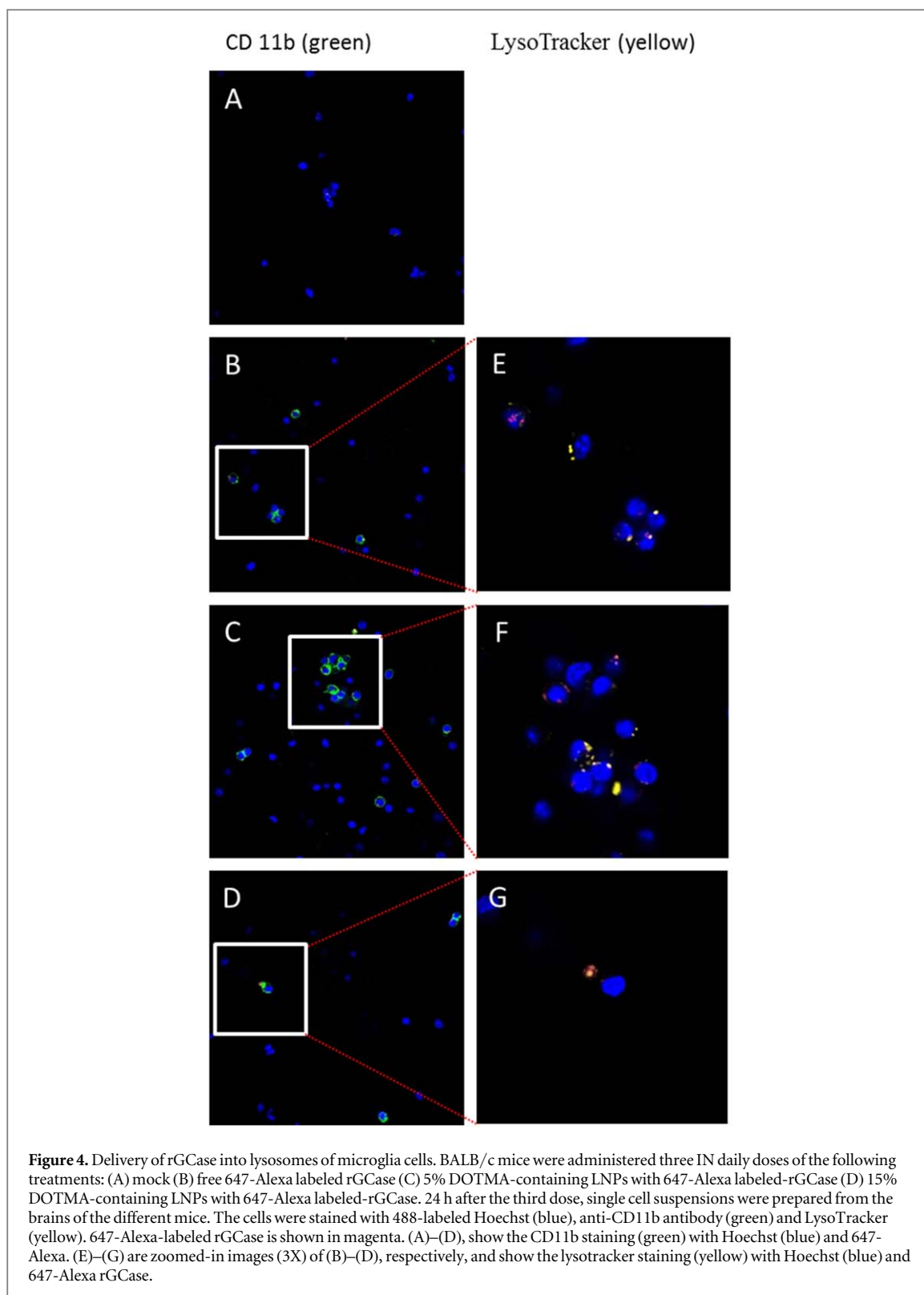
the cellular accumulation of free rGCCase and rGCCase entrapped in LNPs. Mice that were treated with encapsulated rGCCase had a much higher amount of rGCCase than mice that were treated with free rGCCase. These results strongly attest that encapsulating rGCCase in particles has an advantage over free recombinant enzyme when delivered into the brain.

### 3.5. rGCCase-loaded LNPs are able to restore enzymatic activity

In order to ascertain that our delivery strategy can restore enzymatic activity in diseased cells, we incubated the LNPs with human primary skin fibroblasts that derived from severe GD patients. These cells represent the human disease and are used for examining the therapeutic potential of the delivery vehicle. The results demonstrated that only DOTMA-containing LNPs were able to elevate enzymatic activity in the cells by 30%, demonstrating that the encapsulated enzyme was endocytosed into the cells and released in such a manner that it could restore activity of the deficient GD-derived cells (table 2). Taking into consideration that fibroblasts do not possess phagocytic capabilities, the elevation in enzyme activity in the treated primary human cells is within the therapeutic range, which highlights the potential of the DOTMA LNPs as carriers of rGCCase.

## 4. Discussion

In the present study, we tested the feasibility of introducing rGCCase, encapsulated in lipid nanoparticles into the brain. We introduced intranasally free rGCCase or rGCCase entrapped in the LNPs and tested their ability to bypass the BBB and to be endocytosed into brain microglia cells. Our results showed that we have successfully constructed a lipid based delivery strategy for facilitating IN delivery of rGCCase into the brain's parenchyma. We show that the  $\sim$ 200 nm LNPs that we constructed are of an ideal size for cellular delivery and are highly stable and homogenous. When tested *ex vivo*, using brain derived single cell suspensions; all formulations and the free rGCCase were successful in facilitating entrance of rGCCase into CD11b positive microglia cells. *In vivo* biodistribution assessment revealed that LNPs were superior in transporting rGCCase into the brain ( $\sim$ 4% of ID/mg tissue) compare with  $\sim$ 0.3% of ID/mg tissue—representing more than 10-fold difference. The LNPs transported more enzyme into the appropriate therapeutic location within the brain. Our results also demonstrated that the encapsulated GCCase not only entered its target cells, the microglia, but was also detected in their lysosomes, the therapeutic site of the drug. Finally, we demonstrated that the DOTMA-based LNPs could restore enzymatic activity in GCCase deficient cells derived from GD patients.



Several efforts to deliver lysosomal enzymes into the brain have been documented, these included intrathecal and intracerebroventricular administrations. Intrathecal administration was performed in animal models of mucopolysaccharidosis MPS I, II and IIIA, late infantile neuronal ceroid lipofuscinosis, and Niemann–Pick type A. The results indicated distribution of the recombinant enzyme throughout the CNS, with concomitant clearance of accumulated material within the lysosomes [45, 46]. Concerning intracerebroventricular administration, profound improvements at the histopathological and functional level have been reported in animal models of metachromatic leukodystrophy (MLD) following delivery of arylsulfatase A [47]. Intrathecal delivery in MPS I and VI is already in clinical trials [45, 48].

**Table 2.** GCCase activity in cells incubated with different rGCCase formulations. A, B, GD-derived cells (lines GM877 and GM8760, respectively) were incubated with different formulation of rGCCase. Four hours later enzymatic activity was tested using a 4-MUG substrate as described in the Materials and Methods section. (A) Untreated cells, (B) Free rGCCase, (C) LNPs only, (D) LNPs containing DOTMA E-LNPs entrapping rGCCase F- LNPs containing DOTMA entrapping rGCCase. Significance: \*\*  $p < 0.01$ . The results are presented graphically (A) and in a table (B). The results are a summary of five experiments performed in six repeats each  $\pm$  standard error.

Treatment	GM8760 cells	GM877 cells
(A) Untreated cells	100	100
(B) Free GCCase	101.2 $\pm$ 1	103.6 $\pm$ 17
(C) LNPs only	99.4 $\pm$ 0.9	104.2 $\pm$ 20
(D) 15% DOTMA LNPs	97.1 $\pm$ 0.5	103.2 $\pm$ 17
(E) LNPs + GCCase	103 $\pm$ 1.1	103 $\pm$ 20
(F) LNPs + 15% DOTMA + GCCase	131.7 $\pm$ 18**	135 $\pm$ 12**

The use of nanoparticle carriers has already been investigated. Thus, liposomes containing beta-galactosidase injected into a rat tail vein were shown to penetrate the BBB and reach the lysosomes in the CNS tissue more effectively than the free enzyme [49].

The use of antibody or peptide delivery vectors capable of facilitating an enzyme entrance into the brain is also under investigation [50–53]. Thus, delivery of  $\alpha$ -galactosidase into a mouse brain, via the BBB transferrin receptor, was evaluated by enzyme conjugation to the BBB transferrin receptor-specific monoclonal antibody in a rat [52].

The introduction of peptide-linked recombinant lysosomal rGCCase into knock-out neurons resulted in the reduction of approximately 90% of the accumulated lipid substrate glucosylsphingosine [53]. Lysosome-targeted octadecyl-rhodamine B-liposomes were found to enhance the lysosomal accumulation of rGCCase (velaglucerase alfa, SHIRE) for improving lysosomal delivery in GD fibroblasts [54].

An interesting issue is what increase in enzymatic activity would be needed in order for therapy to be efficient; as discussed [55, 56], a mere 1%–5% of normal intracellular enzyme activity was sufficient to correct the metabolic defect in enzyme-deficient cells.

## 5. Conclusion

Herein we showed that specific LNP formulation could be used to deliver rGCCase to its target cells *in vivo* via an IN delivery route. The strategy of targeted delivery and bypassing the BBB may become a novel therapeutic modality to treat neuronopathic GD, and may serve as a platform for other lysosomal storage diseases that involve neuropathic symptoms. Moreover, this strategy may pave the way as a novel therapeutic approach to treat other diseases such as Alzheimer's and Parkinson's.

## Acknowledgments

This work was supported in part by grants from Shire Genetics (Lexington, MA) awarded to MH and DP and by the FTA: Nanomedicines for Personalized Theranostics of the Israeli National Nanotechnology Initiative; and by The Leona M and Harry B Helmsley Nanotechnology Research Fund awarded to DP.

## ORCID iDs

Dan Peer  <https://orcid.org/0000-0001-8238-0673>

## References

- [1] Brady RO, Kanfer JN and Shapiro D 1965 Metabolism of glucocerebrosides: II. Evidence of an enzymatic deficiency in Gaucher's disease *Biochem. Biophys. Res. Commun.* **18** 221–5
- [2] Beutler E and Gelbart T 1996 Glucocerebrosidase (Gaucher disease) *Hum. Mutation* **8** 207–13
- [3] Beutler E 1995 Gaucher disease *Adv. Genet.* **32** 17–49
- [4] Theophilus B, Latham T, Grabowski G A and Smith F I 1989 Gaucher disease: molecular heterogeneity and phenotype-genotype correlations *Am. J. Hum. Genet.* **45** 212–25

- [5] Ginns E I, Brady R O, Pirruccello S, Moore C, Sorrell S, Furbish F S, Murray G J, Tager J and Barranger J A 1982 Mutations of glucocerebrosidase: discrimination of neurologic and non-neurologic phenotypes of Gaucher disease *Proc. Natl Acad. Sci. USA* **79** 5607–10
- [6] Hruska K S, LaMarca M E, Scott C R and Sidransky E 2008 Gaucher disease: mutation and polymorphism spectrum in the glucocerebrosidase gene (GBA) *Hum. Mutation* **29** 567–83
- [7] Erikson A, Bembi B and Schiffmann R 1997 Neuronopathic forms of Gaucher's disease *Baillieres Clin. Haematol.* **10** 711–23
- [8] Weinreb N J et al 2002 Effectiveness of enzyme replacement therapy in 1028 patients with type 1 Gaucher disease after 2 to 5 years of treatment: a report from the Gaucher registry *Am. J. Med.* **113** 112–9
- [9] Weinreb N J, Goldblatt J, Villalobos J, Charrow J, Cole J A, Kerstenetzky M, vom Dahl S and Hollak C 2013 Long-term clinical outcomes in type 1 Gaucher disease following 10 years of imiglucerase treatment *J. Inherit. Metab. Dis.* **36** 543–53
- [10] Barton N W et al 1991 Replacement therapy for inherited enzyme deficiency—macrophage-targeted glucocerebrosidase for Gaucher's disease *New Engl. J. Med.* **324** 1464–70
- [11] Elstein D and Zimran A 2009 Review of the safety and efficacy of imiglucerase treatment of Gaucher disease *Biologics* **3** 407–17
- [12] Xu X, Costa A and Burgess D J 2012 Protein encapsulation in unilamellar liposomes: high encapsulation efficiency and a novel technique to assess lipid-protein interaction *Pharm. Res.* **29** 1919–31
- [13] Colletier J P, Chaize B, Winterhalter M and Fournier D 2002 Protein encapsulation in liposomes: efficiency depends on interactions between protein and phospholipid bilayer *BMC Biotechnol.* **2** 9
- [14] Hirai M, Kimura R, Takeuchi K, Hagiwara Y, Kawai-Hirai R, Ohta N, Igarashi N and Shimizu N 2013 Structure of liposome encapsulating proteins characterized by x-ray scattering and shell-modeling *J. Synchrotron Radiat.* **20** 869–74
- [15] des Rieux A, Fievez V, Garinot M, Schneider Y J and Preat V 2006 Nanoparticles as potential oral delivery systems of proteins and vaccines: a mechanistic approach *J. Control. Release* **116** 1–27
- [16] Peer D, Karp J M, Hong S, Farokhzad O C, Margalit R and Langer R 2007 Nanocarriers as an emerging platform for cancer therapy *Nat. Nanotechnol.* **2** 751–60
- [17] Lim S B, Banerjee A and Onyuksek H 2012 Improvement of drug safety by the use of lipid-based nanocarriers *J. Control. Release* **163** 34–45
- [18] Peer D, Park E J, Morishita Y, Carman C V and Shimaoka M 2008 Systemic leukocyte-directed siRNA delivery revealing cyclin D1 as an anti-inflammatory target *Science* **319** 627–30
- [19] Bondi M L, Di Gesu R and Craparo E F 2012 Lipid nanoparticles for drug targeting to the brain *Methods Enzymol.* **508** 229–51
- [20] Hernandez-Pedro N Y, Rangel-Lopez E, Magana-Maldonado R, de la Cruz V P, del Angel A S, Pineda B and Sotelo J 2013 Application of nanoparticles on diagnosis and therapy in gliomas *Biomed. Res. Int.* **2013** 351031
- [21] Soppimath K S, Aminabhavi T M, Kulkarni A R and Rudzinski W E 2001 Biodegradable polymeric nanoparticles as drug delivery devices *J. Control. Release* **70** 1–20
- [22] Al-Jamal W T and Kostarelos K 2011 Liposomes: from a clinically established drug delivery system to a nanoparticle platform for theranostic nanomedicine *Acc. Chem. Res.* **44** 1094–104
- [23] Chapman C D, Frey W H 2nd, Craft S, Danielyan L, Hallschmid M, Schiöth H B and Benedict C 2013 Intranasal treatment of central nervous system dysfunction in humans *Pharm. Res.* **30** 2475–84
- [24] Poulos A and Pollard A C 1976 A rapid method for the estimation of beta-galactocerebrosidase, beta-glucocerebrosidase and sphingomyelinase activities in leukocytes *Clin. Chim. Acta* **72** 327–35
- [25] Beutler E 2004 Enzyme replacement in Gaucher disease *PLoS Med.* **1** e21
- [26] Vitner E B, Farfel-Becker T, Eilam R, Biton I and Futerman A H 2012 Contribution of brain inflammation to neuronal cell death in neuronopathic forms of Gaucher's disease *Brain* **135** 1724–35
- [27] Kelly C, Jefferies C and Cryan S A 2011 Targeted liposomal drug delivery to monocytes and macrophages *J. Drug Deliv.* **2011** 727241
- [28] Frenz T, Grabski E, Durán V, Hozsa C, Stepczyńska A, Furch M, Gieseler R K and Kalinke U 2015 Antigen presenting cell-selective drug delivery by glycan-decorated nanocarriers *Eur. J. Pharm. Biopharm.* **95** 13–7
- [29] Cohen K, Emmanuel R, Kisin-Finifer E, Shabat D and Peer D 2014 Modulation of drug resistance in ovarian adenocarcinoma using chemotherapy entrapped in hyaluronan-grafted nanoparticle clusters *ACS Nano* **8** 2183–95
- [30] Bachar G, Cohen K, Hod R, Feinmesser R, Mizrahi A, Shpitzer T, Katz O and Peer D 2011 Hyaluronan-grafted particle clusters loaded with Mitomycin C as selective nanovectors for primary head and neck cancers *Biomaterials* **32** 4840–8
- [31] Chatin B et al 2015 Liposome-based formulation for intracellular delivery of functional proteins *Mol. Ther. Nucleic Acids* **4** e244
- [32] Huang W J, Zhang X and Chen W W 2015 Gaucher disease: a lysosomal neurodegenerative disorder *Eur. Rev. Med. Pharmacol. Sci.* **19** 1219–26
- [33] Bigdeli A, Palchetti S, Pozzi D, Hormozi-Nezhad M R, Baldelli Bombelli F, Caracciolo G and Mahmoudi M 2016 Exploring cellular interactions of liposomes using protein corona fingerprints and physicochemical properties *ACS Nano* **10** 3723–37
- [34] Wolfram J, Suri K, Yang Y, Shen J, Celia C, Fresta M, Zhao Y, Shen H and Ferrari M 2014 Shrinkage of pegylated and non-pegylated liposomes in serum *Colloids Surf. B* **114** 294–300
- [35] Sato Y and Beutler E 1993 Binding, internalization, and degradation of mannose-terminated glucocerebrosidase by macrophages *J. Clin. Invest.* **91** 1909–17
- [36] Born J, Lange T, Kern W, McGregor G P, Bickel U and Fehm H L 2002 Sniffing neuropeptides: a transnasal approach to the human brain *Nat. Neurosci.* **5** 514–6
- [37] Chen X Q, Fawcett J R, Rahman Y E, Ala T A and Frey I W 1998 Delivery of nerve growth factor to the brain via the olfactory pathway *J. Alzheimers Dis.* **1** 35–44
- [38] Thorne R G, Hanson L R, Ross T M, Tung D and Frey W H 2nd 2008 Delivery of interferon-beta to the monkey nervous system following intranasal administration *Neuroscience* **152** 785–97
- [39] Thorne R G, Pronk G J, Padmanabhan V and Frey W H 2nd 2004 Delivery of insulin-like growth factor-I to the rat brain and spinal cord along olfactory and trigeminal pathways following intranasal administration *Neuroscience* **127** 481–96
- [40] Illum L 2004 Is nose-to-brain transport of drugs in man a reality? *J. Pharm. Pharmacol.* **56** 3–17
- [41] Yang J P, Liu H J, Cheng S M, Wang Z L, Cheng X, Yu H X and Liu X F 2009 Direct transport of VEGF from the nasal cavity to brain *Neurosci. Lett.* **449** 108–11
- [42] De Rosa R, Garcia A A, Braschi C, Capsoni S, Maffei L, Berardi N and Cattaneo A 2005 Intranasal administration of nerve growth factor (NGF) rescues recognition memory deficits in AD11 anti-NGF transgenic mice *Proc. Natl Acad. Sci. USA* **102** 3811–6
- [43] Ross T M, Martinez P M, Renner J C, Thorne R G, Hanson L R and Frey W H 2nd 2004 Intranasal administration of interferon beta bypasses the blood-brain barrier to target the central nervous system and cervical lymph nodes: a non-invasive treatment strategy for multiple sclerosis *J. Neuroimmunol.* **151** 66–77

- [44] Jitendra, Sharma P K, Bansal S and Banik A 2011 Noninvasive routes of proteins and peptides drug delivery *Indian J. Pharm. Sci.* **73** 367–75
- [45] Dickson P I 2009 Novel treatments and future perspectives: outcomes of intrathecal drug delivery *Int. J. Clin. Pharmacol. Ther.* **47** (Suppl. 1) S124–7
- [46] Kakkis E, McEntee M, Vogler C, Le S, Levy B, Belichenko P, Mobley W, Dickson P, Hanson S and Passage M 2004 Intrathecal enzyme replacement therapy reduces lysosomal storage in the brain and meninges of the canine model of MPS I *Mol. Genet. Metab.* **83** 163–74
- [47] Stroobants S, Gerlach D, Matthes F, Hartmann D, Fogh J, Gieselmann V, D'Hooge R and Matzner U 2011 Intracerebroventricular enzyme infusion corrects central nervous system pathology and dysfunction in a mouse model of metachromatic leukodystrophy *Hum. Mol. Genet.* **20** 2760–9
- [48] Dickson P I and Chen A H 2011 Intrathecal enzyme replacement therapy for mucopolysaccharidosis: I. Translating success in animal models to patients *Curr. Pharm. Biotechnol.* **12** 946–55
- [49] Hitoshio Noderag O A, Tada E and Desnic R J 1983 Microautoradiographic study on the localization of liposome-entrapped 3H-labeled p-galactosidase injected tissue or untrapped into rats *Tohoku J. Exp. Med.* 1–13
- [50] Wang D, El-Amouri S S, Dai M, Kuan C Y, Hui D Y, Brady R O and Pan D 2013 Engineering a lysosomal enzyme with a derivative of receptor-binding domain of apoE enables delivery across the blood–brain barrier *Proc. Natl Acad. Sci. USA* **110** 2999–3004
- [51] Bockenhoff A, Cramer S, Wolte P, Knieling S, Wohlenberg C, Gieselmann V, Galla H J and Matzner U 2014 Comparison of five peptide vectors for improved brain delivery of the lysosomal enzyme arylsulfatase A *J. Neurosci.* **34** 3122–9
- [52] Zhang Y and Pardridge W M 2005 Delivery of beta-galactosidase to mouse brain via the blood–brain barrier transferrin receptor *J. Pharmacol. Exp. Ther.* **313** 1075–81
- [53] Gramlich P A *et al* 2016 A peptide-linked recombinant glucocerebrosidase for targeted neuronal delivery: design, production, and assessment *J. Biotechnol.* **221** 1–12
- [54] Thekkedath R, Koshkaryev A and Torchilin V P 2013 Lysosome-targeted octadecyl-rhodamine B-liposomes enhance lysosomal accumulation of glucocerebrosidase in Gaucher's cells *in vitro Nanomedicine* **8** 1055–65
- [55] Desnick R J and Schuchman E H 2002 Enzyme replacement and enhancement therapies: lessons from lysosomal disorders *Nat. Rev. Genet.* **3** 954–66
- [56] Desnick R J and Schuchman E H 2012 Enzyme replacement therapy for lysosomal diseases: lessons from 20 years of experience and remaining challenges *Annu. Rev. Genom. Hum. Genet.* **13** 307–35